Title
Towards spatial frequency domain optical imaging of neurovascular coupling in a mouse model of Alzheimer's disease

ISBN
9780819488503

Authors
Lin, Alexander J
Konecky, Soren D
Rice, Tyler B
et al.

Publication Date
2012-02-03

DOI
10.1117/12.907557

Towards spatial frequency domain optical imaging of neurovascular coupling in a mouse model of Alzheimer's disease

Alexander J. Lin[1], Soren D. Konecky[1] , Tyler B. Rice[1], Kim N. Green[2], Bernard Choi[1], Anthony J. Durkin[1], Bruce J. Tromberg[1]

[1] Beckman Laser Institute and Medical Clinic, University of California, Irvine

[2] Department of Neurobiology and Behavior, University of California, Irvine

ABSTRACT

Early neurovascular coupling (NVC) changes in Alzheimer's disease can potentially provide imaging biomarkers to assist with diagnosis and treatment. Previous efforts to quantify NVC with intrinsic signal imaging have required assumptions of baseline optical pathlength to calculate changes in oxy- and deoxy-hemoglobin concentrations during evoked stimuli. In this work, we present an economical spatial frequency domain imaging (SFDI) platform utilizing a commercially available LED projector, camera, and off-the-shelf optical components suitable for imaging dynamic optical properties. The fast acquisition platform described in this work is validated on silicone phantoms and demonstrated in neuroimaging of a mouse model.

Keywords: optical properties, LED microprojector

INTRODUCTION

Alzheimer's disease (AD) is a neurodegenerative disease affecting 35 million people worldwide. [1]. There is significant interest in developing in vivo imaging methods for AD to enhance our understanding of the disease and to help facilitate earlier intervention [2, 3]. Most AD cases (60-90%) are associated with ischemic vascular disease, and 90% of AD patients exhibit cerebral amyloid angiopathy (CAA), a vascular disease caused by amyloid deposition in the vessels[1]. A physiological consequence of CAA, reduced vascular reactivity, has been shown in Alzheimer's using transcranial doppler [4-6], fMRI [7, 8], PET [9], and SPECT [10] techniques. Neurovascular coupling (NVC), the localized vasodilation that occurs from a specific metabolic demand, is also reduced in AD with visual [11] and verbal fluency[12] challenges. Therefore, development of imaging biomarkers sensitive to these potentially early physiological changes is of great interest.

Rodent models of AD are useful for studying the time course of pathology. In the triple transgenic (3xTg-AD) mouse model of AD, we have shown significant baseline absorption and scattering contrast in the near-infrared wavelengths (650-970nm) as well as magnitude differences in brain oxygenation to an inhaled-hyperoxia challenge in severely pathological mice compared to controls [13]. Others have also seen neurovascular decoupling in a CAA mouse model with laser speckle imaging [14]. NVC has largely been studied in rats with intrinsic signal imaging, which relies on the modified Beer-Lambert law (Eq. 1) to fit oxy- and deoxy-hemoglobin concentration changes from reflectance changes at two or more wavelengths of light.

$$\Delta A(\lambda) = \sum (E(\lambda) * \Delta c * D(\lambda)) \qquad \text{(Eq. 1)}$$

Where $\Delta A(\lambda)$ is the wavelength-dependent log of the normalized change in reflectance, $E(\lambda)$ is the wavelength-dependent extinction coefficient of chromophore c, and $D(\lambda)$ is the path length traveled which depends on

Photonic Therapeutics and Diagnostics VIII, edited by Nikiforos Kollias, et al., Proc. of SPIE Vol. 8207, 82074U

absorption and scattering coefficients of the tissue. These absorption and scattering coefficients are usually assumed a priori, but doing so when comparing AD to control mice with differing baseline optical properties can lead to calculation errors.

Spatial frequency domain imaging (SFDI) is a reflectance based imaging technique that can avoid assumptions regarding intrinsic signal detection by resolving absorption and scattering coefficients in tissue on a pixel-by-pixel basis. SFDI works by structuring light into sinusoidal patterns and projecting them onto the tissue surface [15]. The tissue acts a spatial filter and blurs the structured patterns. By projecting patterns of differing spatial frequencies, the Modulation Transfer Function (MTF) of the tissue can be found which uniquely determines a pair of optical absorption and scattering coefficients. Spectroscopic measurements made at wavelengths ranging from 650 to 970nm are used to determine intrinsic concentrations of oxy- and deoxy-hemoglobin, water, and lipid [16, 17]. Spatial resolution is dependent on the field-of-view and number of pixels in the CCD camera, while temporal resolution for acquiring a series of spectroscopic maps can vary from seconds to minutes depending on the wavelength selection strategy [18]. In this paper, an SFDI system is described that is optimized for quantitatively detecting the fast and small intrinsic signals we expect to observe during an evoked stimulus test of NVC.

METHODS

Instrumentation: We modified an LED microprojector (M2, *AAXA Technologies*) to project a field-of-view of 17x22mm by removing the lens array and replacing the tube lens with a 100mm collimating and 400mm focusing lens (*Thorlabs*). In this work the blue LED was disconnected, while leaving the green and red LEDs centered at 525nm and 623nm, respectively (Fig. 1). We measured the liquid crystal on silicone (LCoS) chip in the Aaxa refresh rate at 350Hz and sequential display of a single color frame in the pattern RGBGR, essentially giving a total refresh rate of 70Hz, or about 14.286ms/frame. Thus we used multiples of 14.286ms as the exposure time to get consistent light levels. The gray scale of the projector was also non-linear and had to be determined empirically by averaging the camera response to calibration projections (Fig. 1). From the calibration, we are able to project corrected sinusoidal patterns onto the sample and, as seen in Figure 2, the reflected image is separated spectrally with a dichroic (*Omega*) and further bandpass-filtered (FB530-10, FL632.8-10, *Thorlabs*) before hitting two 12-bit CCD cameras (Flea2G, *Pointgrey*). Images from the two cameras were coregistered by using a fiduciary marker on a phantom[19] (Fig. 2). Linear polarizers (47315, *Edmund Optics*) were also put before each camera to reduce specular reflection from the sample. The projector and cameras were connected to a PC and controlled by custom Labview software (*National Instruments*).

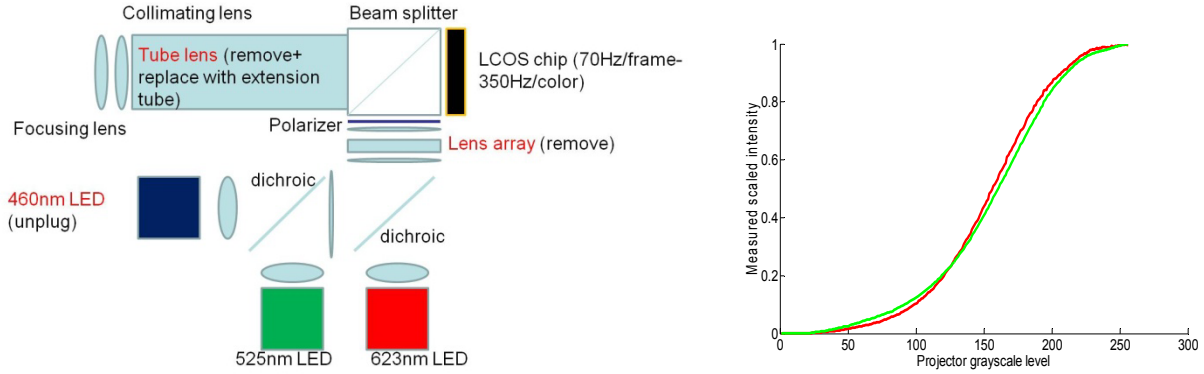

Figure 1: (Left) Block diagram of AAXA M2 microprojector modifications. (Right) Gamma functions for green and red channels of AAXA M2 microprojector.

Phantom experiments: Optical properties of a silicone phantom were calculated using a rapid lookup-table approach described in [16]. We derived reflectance at two frequencies by projecting three sinusoid patterns 120 degrees out of phase sequentially. The remitted reflectance was captured by the two cameras and saved for further processing offline (Eq. 2, 3). Camera dark images were also acquired to subtract for proper reflectance calibration.

The average acquisition time for two wavelengths and two frequencies was less than 1.5 seconds, faster than any SFDI instrument currently employed. Reflectance at the two spatial frequencies was calculated using

$$R_{DC} = (I_1+I_2+I_3)/3 - I_{dark} \quad \text{(Eq. 2)}$$

$$R_{AC} = (2\text{^}0.5/3) * ((I_1-I_2)\text{^}2 + (I_1-I_3)\text{^}2 + (I_2-I_3)\text{^}2)\text{^}0.5, \quad \text{(Eq. 3)}$$

where R_{DC} and R_{AC} are the reflectance at zero and high frequency, respectively. I_1, I_2, I_3 are the three captured images at the three different phases and I_{dark} is the dark image. Optimal spatial frequencies remain to be seen, but ranges from 0.1-0.3mm^{-1} were tested. Stability tests were conducted by taking data at 1.5s/acquisition for 30 minutes. Using the accepted paradigm for intrinsic signal imaging of averaging many block trials to get an average neurovascular coupling response, we averaged 60 thirty second "trials" to see the sensitivity to change in reflectance and optical properties in our imaging system.

Mouse experiment: We imaged a one-month old C57/Bl6 mouse under 1% isoflurane anesthesia. We removed the skin above the scalp and created a vasoline well filled with sterile saline and covered with a glass coverslip to induce optical transparency of the thin skull of a young mouse. Optical properties were determined from SFDI at 530 and 633nm, projecting at 0.3mm^-1 frequency. All procedures were performed in accordance with the regulations of the Institutional Animal Care and Use Committee (IACUC) of the University of California, Irvine (protocol no. 2010-2934).

RESULTS

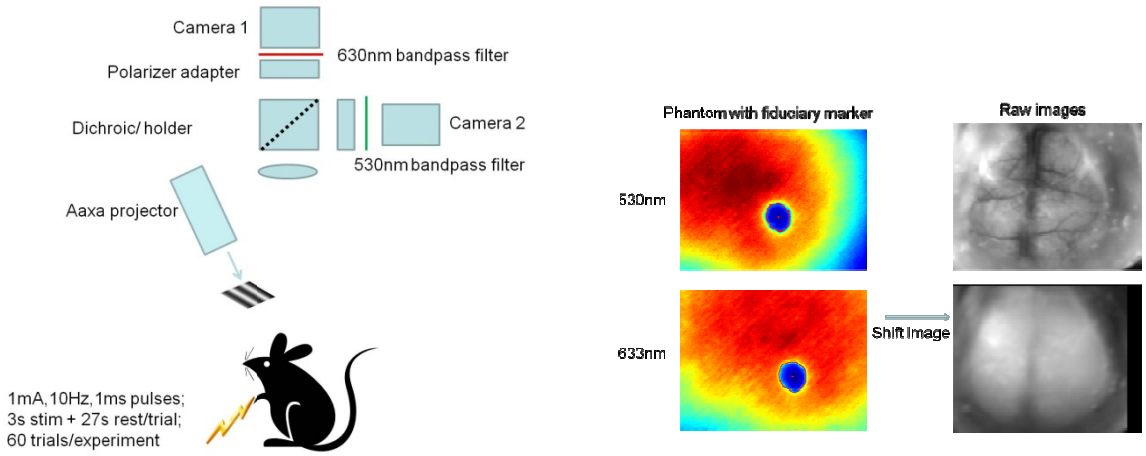

Figure 2: (Left) Block diagram of fast SFDI setup. (Right) Coregistration of images from the two cameras using a fiduciary marker.

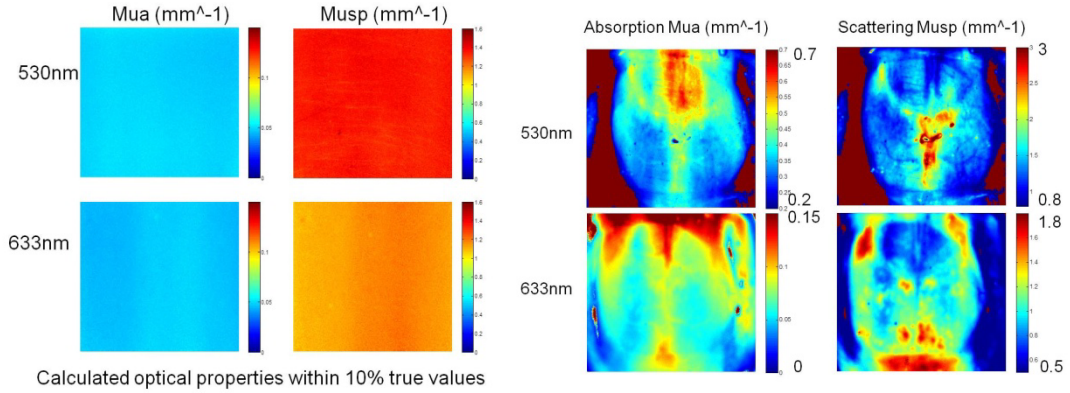

Figure 3: (Left) Phantom optical properties were acquired and were within 10% of true values. (Right) Baseline optical properties from a mouse brain in vivo. Average and standard deviation of μ_a and μ_s' in the whole cortex at 530nm were 0.421 ± 0.080mm^-1 and 1.52 ± 0.38mm^-1, respectively, and μ_a and μ_s' at 633nm were 0.082 ± 0.027mm^-1 and 1.03 ± 0.21mm^-1, respectively. A two-wavelength fit for total hemoglobin values gave an average and standard deviation value of 46.9 ± 8.9μM in the one-month old control mouse cortex.

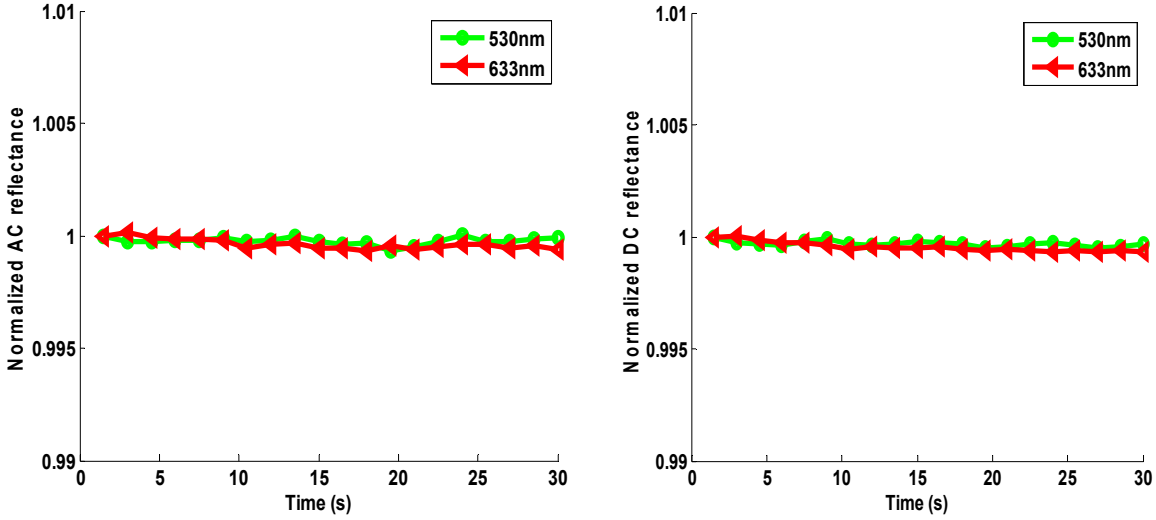

Figure 4: (Left) Normalized average AC reflectance and (Right) normalized average DC reflectance over 30 seconds showing under 0.1% drift when averaged over 60 trials.

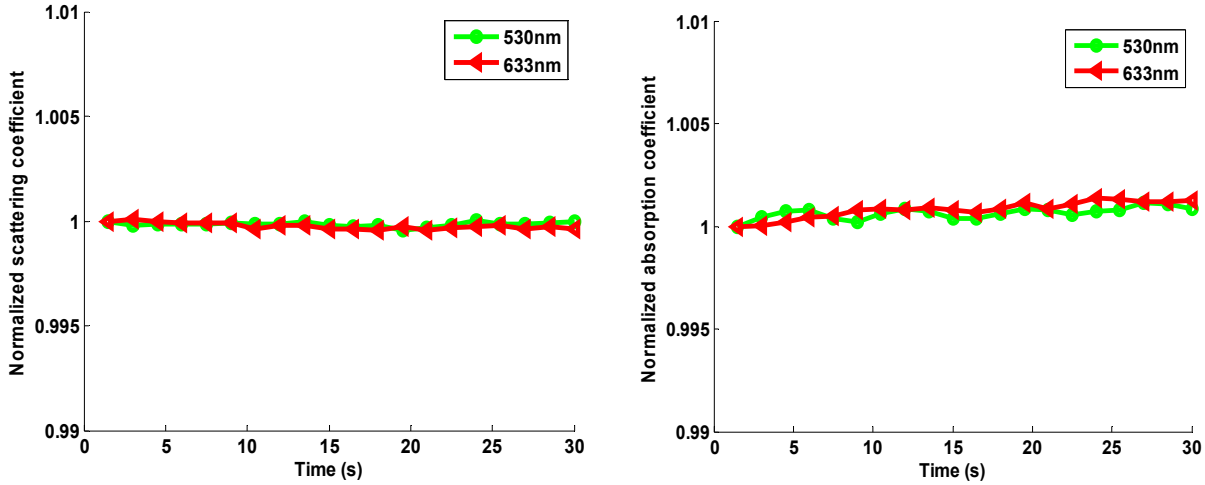

Figure 5: (Left) Normalized average scattering coefficient and (Right) normalized average absorption coefficient over 30 seconds showing under 0.2% drift when averaged over 60 trials.

CONCLUSIONS

It is difficult to study AD as it is currently a diagnosis of exclusion that requires cognitive impairment and a certain level of amyloid-beta plaques, typically found during autopsy. Therefore, in vivo imaging biomarkers that can probe the anatomical and physiological changes in early AD would be invaluable to the diagnosis and treatment of AD. Neurovascular uncoupling may be an early pathological marker of AD, but current intrinsic imaging studies in rodent models lack an imaging method capable of accounting for baseline optical property differences. This fast SFDI platform is optimized for quantitatively detecting small changes in scattering and absorption that are necessary for measuring the vascular response during evoked stimuli. These measurements may lead to earlier sequencing of the uncoupling process in an AD mouse model and suggest a novel early biomarker for testing in humans with analogous transcranial NIRS techniques.

ACKNOWLEDGEMENTS

Funding for this work was supported by the NIH Laser and Microbeam Medical Program (LAMMP P41-RR01192) , NIH/NIA Ruth L. Kirschtein National Research Service Award (F30), American Society for Laser Medicine and Surgery student grant, NIH-funded UC Irvine Medical Scientist Training Program (MSTP), and the Beckman Foundation.

REFERENCES

[1] Querfurth, H. W., and LaFerla, F. M., "Alzheimer's disease," *N Engl J Med,* vol. 362, no. 4, pp. 329-44, (2010).

[2] Klunk, W. E., Engler, H., Nordberg, A. *et al.*, "Imaging brain amyloid in Alzheimer's disease with Pittsburgh Compound-B," *Ann Neurol,* vol. 55, no. 3, pp. 306-19, (2004).

[3] Price, J. L., McKeel, D. W., Jr., Buckles, V. D. *et al.*, "Neuropathology of nondemented aging: presumptive evidence for preclinical Alzheimer disease," *Neurobiol Aging,* vol. 30, no. 7, pp. 1026-36, (2009).

[4] Vicenzini, E., Ricciardi, M. C., Altieri, M. *et al.*, "Cerebrovascular reactivity in degenerative and vascular dementia: a transcranial Doppler study," *Eur Neurol,* vol. 58, no. 2, pp. 84-9, (2007).

[5] Silvestrini, M., Pasqualetti, P., Baruffaldi, R. *et al.*, "Cerebrovascular reactivity and cognitive decline in patients with Alzheimer disease," *Stroke,* vol. 37, no. 4, pp. 1010-5, (2006).

[6] Stefani, A., Sancesario, G., Pierantozzi, M. *et al.*, "CSF biomarkers, impairment of cerebral hemodynamics and degree of cognitive decline in Alzheimer's and mixed dementia," *J Neurol Sci,* vol. 283, no. 1-2, pp. 109-15, (2009).
[7] Yezhuvath, U. S., Uh, J., Cheng, Y. *et al.*, "Forebrain-dominant deficit in cerebrovascular reactivity in Alzheimer's disease," *Neurobiol Aging*, (2012).
[8] Kassner, A., Winter, J. D., Poublanc, J. *et al.*, "Blood-oxygen level dependent MRI measures of cerebrovascular reactivity using a controlled respiratory challenge: reproducibility and gender differences," *J Magn Reson Imaging,* vol. 31, no. 2, pp. 298-304, (2010).
[9] Stoppe, G., Schutze, R., Kogler, A. *et al.*, "Cerebrovascular reactivity to acetazolamide in (senile) dementia of Alzheimer's type: relationship to disease severity," *Dementia,* vol. 6, no. 2, pp. 73-82, (1995).
[10] Pavics, L., Grunwald, F., Reichmann, K. *et al.*, "rCBF SPECT and the acetazolamide test in the evaluation of dementia," *Nucl Med Rev Cent East Eur,* vol. 1, no. 1, pp. 13-9, (1998).
[11] Zeller, J. B., Herrmann, M. J., Ehlis, A. C. *et al.*, "Altered parietal brain oxygenation in Alzheimer's disease as assessed with near-infrared spectroscopy," *Am J Geriatr Psychiatry,* vol. 18, no. 5, pp. 433-41, (2010).
[12] Herrmann, M. J., Langer, J. B., Jacob, C. *et al.*, "Reduced prefrontal oxygenation in Alzheimer disease during verbal fluency tasks," *Am J Geriatr Psychiatry,* vol. 16, no. 2, pp. 125-35, (2008).
[13] Lin, A. J., Koike, M. A., Green, K. N. *et al.*, "Spatial frequency domain imaging of intrinsic optical property contrast in a mouse model of Alzheimer's disease," *Ann Biomed Eng,* vol. 39, no. 4, pp. 1349-57, (2011).
[14] Shin, H. K., Jones, P. B., Garcia-Alloza, M. *et al.*, "Age-dependent cerebrovascular dysfunction in a transgenic mouse model of cerebral amyloid angiopathy," *Brain,* vol. 130, no. Pt 9, pp. 2310-9, (2007).
[15] Cuccia, D. J., Bevilacqua, F., Durkin, A. J. *et al.*, "Modulated imaging: quantitative analysis and tomography of turbid media in the spatial-frequency domain," *Opt Lett,* vol. 30, no. 11, pp. 1354-6, (2005).
[16] Cuccia, D. J., Bevilacqua, F., Durkin, A. J. *et al.*, "Quantitation and mapping of tissue optical properties using modulated imaging," *J Biomed Opt,* vol. 14, no. 2, pp. 024012, (2009).
[17] Mazhar, A., Dell, S., Cuccia, D. J. *et al.*, "Wavelength optimization for rapid chromophore mapping using spatial frequency domain imaging," *J Biomed Opt,* vol. 15, no. 6, pp. 061716, (2010).
[18] Weber, J. R., Cuccia, D. J., Johnson, W. R. *et al.*, "Multispectral imaging of tissue absorption and scattering using spatial frequency domain imaging and a computed-tomography imaging spectrometer," *J Biomed Opt,* vol. 16, no. 1, pp. 011015, (2011).
[19] Nguyen, J. Q., Saager, R. B., Cuccia, D. J. *et al.*, "Effects of motion on optical properties in the spatial frequency domain," *J Biomed Opt,* vol. 16, no. 12, pp. 126009, (2011).